Obstacle Avoidance During Walking in Real and Virtual Environments

PHILIP W. FINK
Florida Atlantic University
PATRICK S. FOO
University of North Carolina at Asheville
and
WILLIAM H. WARREN
Brown University

Immersive virtual environments are a promising research tool for the study of perception and action, on the assumption that visual–motor behavior in virtual and real environments is essentially similar. We investigated this issue for locomotor behavior and tested the generality of Fajen and Warren's [2003] steering dynamics model. Participants walked to a stationary goal while avoiding a stationary obstacle in matched physical and virtual environments. There were small, but reliable, differences in locomotor paths, with a larger maximum deviation ($\Delta = 0.16$ m), larger obstacle clearance ($\Delta = 0.16$ m), and slower walking speed ($\Delta = 0.13$ m/s) in the virtual environment. Separate model fits closely captured the mean virtual and physical paths ($R^2 > 0.98$). Simulations implied that the path differences are not because of walking speed or a 50% distance compression in virtual environments, but might be a result of greater uncertainty about the egocentric location of virtual obstacles. On the other hand, paths had similar shapes in the two environments with no difference in median curvature and could be modeled with a single set of parameter values ($R^2 > 0.95$). Fajen and Warren's original parameters successfully generalized to new virtual and physical object configurations ($R^2 > 0.95$). These results justify the use of virtual environments to study locomotor behavior.

Categories and Subject Descriptors: J.4 [**Computer Applications**]: Social and Behavioral Sciences—*Psychology*

General Terms: Verification, Experimentation, Theory

Additional Key Words and Phrases: Locomotion, virtual reality, modeling

ACM Reference Format:

Fink, P. W., Foo, P. S., and Warren, W. H. 2007. Obstacle avoidance during walking in real and virtual environments. ACM Trans. Appl. Percpt. 4, 1, Article 2 (January 2007), 18 pages. DOI = 10.1145/1227134.1227136 http://doi.acm.org/10.1145.1227134.1227136

1. INTRODUCTION

Virtual reality technology offers a tool for the study of human perception and action that researchers in the field have long sought. It allows us to break the laws of physics and optics in order to test

Authors' addresses: Philip W. Fink, Center for Complex Systems and Brain Sciences., Florida Atlantic University, Boca Raton, Florida 33431; Patrick S. Foo, Department of Psychology, University of North Carolina at Asheville, Asheville, North Cardina 28801; William H. Warren, Department of Cognitive and Linguistic Sciences, Brown University, Providence, Rhode Island 02912.

hypotheses about perceptually guided action, by manipulating the environment and visual information during ongoing behavior [Tarr and Warren 2002]. It also permits us to dispense with explicit judgment tasks such as magnitude estimation, forced choice, or open-loop visually directed action, and to measure on-line visually controlled action in process. Thus, virtual environments present the opportunity to bring naturalistic visual–motor behavior into the laboratory and study it experimentally, with informational manipulations and proper controls. In particular, ambulatory virtual environments in which the participant can walk freely while wearing a head-mounted display (HMD) provide a new tool with which theories of visually guided locomotion can be rigorously tested.

1.1 Perception in Virtual Environments

This enthusiasm is predicated on the assumption that visual–motor behavior in immersive virtual environments is essentially the same as it is in the real world. There are reasons for caution on this score. For example, when reaching to grasp an object, once the participant discovers that the object is virtual, through lack of haptic feedback, grasp characteristics change to resemble a pantomimed version [Opitz et al. 1996]. This raises the question of whether the mere knowledge that one is viewing a virtual environment can alter visual–motor behavior.

It is frequently observed that the perceived scale of virtual space is inaccurate, even under full visual information conditions. In an extreme illustration of this point participants do not notice the gradual expansion of a textured virtual room about the eye point by up to 200%, even though accurate binocular disparity and motion parallax are available [Glennerster et al. 2006]. Size judgments at 3 and 6 m are dominated by the size of the test object relative to the room, although judgments at near distances (1.5 m) are dominated by disparity and motion. Motion parallax appears to provide only weak information for absolute scale in both real and virtual environments [Beall et al. 1995]. However, since eye height-scaled relative size information remained present in the wall texture in these experiments, even when the floor and ceiling were removed, such results are consistent with the proposal that size perception in virtual environments may be largely determined by information that specifies object size as a proportion of the background and/or the simulated eye height [Sedgwick 1980; Warren and Whang 1987; Dixon et al. 2000]. This would imply that when participants have difficulty establishing their eye height in the scene, this may yield a virtual environment with an ambiguous scale.

Moreover, perceived egocentric distance appears to be systematically biased in virtual environments, as measured in visually directed "blind-walking" tasks. Performance is highly accurate over distances of 2 to 25 m in real environments, but it has been repeatedly found that distance is underestimated by approximately 50% in virtual environments [Loomis and Knapp 2003; Thompson et al. 2004]. Comparable underestimation is observed for both blind walking and blind throwing of a beanbag to a previously viewed target in a virtual hallway [Sahm et al. 2005], indicating that the effect is likely as a result of perceived distance rather than to a bias in spatial updating during blind walking, or to an action-specific visual–motor calibration. Note that such a distance compression would predict a perceptual expansion of the virtual world in depth as the observer walks through it.

Thompson and his colleagues [Thompson et al. 2004; Creem-Regehr et al. 2005] have systematically ruled out explanations of distance underestimation based on graphics quality, occlusion of the feet, absence of disparity and motion parallax, or a restricted field of view (as long as head rotation is permitted). Given that perceived distance along the ground appears to be based on the declination angle of the target [Philbeck 1997; Ooi et al. 2001], the perceived distance compression could be because of a downward bias in sensed gaze angle, a frontal bias in the perceived slant of the ground plane, and/or an underestimation of eye height in virtual environments. Consistent with this interpretation, Willemsen et al. [2004] found that the added forward mass of an HMD accounts for over one-third of the distance

compression, although Messing and Durgin [2005] failed to find the expected effects of a gaze-angle bias. Fortunately for researchers, Mohler et al. [2006] recently reported that this distance underestimation is nearly abolished by 5–7 minutes of walking to targets in a virtual hallway with continuous visual feedback. Thus, locomotor distance appears to adapt quickly in virtual environments, either through a rescaling of perceived distance or a perceptual-motor recalibration.

1.2 Perception and Action

There is reason to question whether explicit judgments, such as visually directed blind walking are good predictors of on-line visually controlled action. Visual judgments and visual behavior that seem to be based on a common perceptual space may actually be task-specific, in that they depend on different environmental properties, informational variables, or perceptual–motor processes [Milner and Goodale 1995]. A case in point is recent research on reaching to grasp a visual illusion, such as the Ebbinghaus illusion. Despite the illusion that one of two equal circles is larger than the other, the hand aperture during an actual grasping movement is relatively unaffected by the illusion [Aglioti et al. 1995; Glover and Dixon 2001; Smeets et al. 2003], although this finding remains controversial [Franz et al. 2000; Franz 2003]. In one analysis, the reported dissociation between perception and action results from a task-specific reliance on the absolute egocentric positions of object edges to control grasping, in contrast to a reliance on relative exocentric extents in spatial perception [Smeets and Brenner 1999; Vishton et al. 1999]. It is likely that similar differences between perceptual judgments and visually controlled actions may occur in virtual environments. This possibility leads us to conclude that to evaluate virtual reality as a research tool for perception and action, one must directly test perceptual–motor behavior. Specifically, validation studies are needed that compare the same visually controlled behavior in matched real and virtual environments. To our knowledge, this has not yet been attempted for legged locomotion. The purpose of the present experiment was to perform such a validation study for the task of obstacle avoidance when walking to a goal.

1.3 A Dynamical Model of Locomotor Path Formation

The study was carried out as part of a program of research on the behavioral dynamics of human locomotion, inspired by the work of Schöner et al. [1995] on a control system for mobile robots. By *behavioral dynamics* we mean the time-evolution of observed behavior, which for locomotor paths can be parameterized by the direction of travel (heading) and its rate of change (turning rate). We hypothesize that locomotion can be decomposed into (at least) four elementary behaviors, including (a) steering toward a stationary target, (b) avoiding a stationary obstacle, (c) intercepting a moving target, and (d) avoiding a moving obstacle. The goal of the research is to specify a dynamical model of each basic behavior and then to determine whether locomotion in increasingly complex environments can be predicted by the linear combination of these components with fixed parameters.

Consider an agent steering to a stationary goal. The current heading direction ϕ (defined with respect to an exocentric reference axis) and the turning rate $\dot{\phi}$ determine the *state space* of the system, assuming a constant speed of travel v (see Figure 1). From the agent's current (x, z) position, a goal lies in the direction ψ_g at a distance d_g; an obstacle may also lie in direction ψ_o at a distance d_o. The simplest description of steering toward a goal is for the agent to bring the target-heading angle (the heading error) to zero ($\phi - \psi_g = 0$). This defines an *attractor* in state space at $(\phi, \dot{\phi}) = (\psi_g, 0)$. Conversely, the simplest description of obstacle avoidance is to increase the obstacle-heading angle ($\phi - \psi_o > 0$), which defines a *repeller* in state space at $(\phi, \dot{\phi}) = (\psi_o, 0)$. In addition, the distance of a goal or obstacle (or equivalently, its time-to-contact) might also be expected to influence steering, because the agent must turn faster to hit a nearer goal or to avoid a nearer obstacle. The problem is to formalize a system

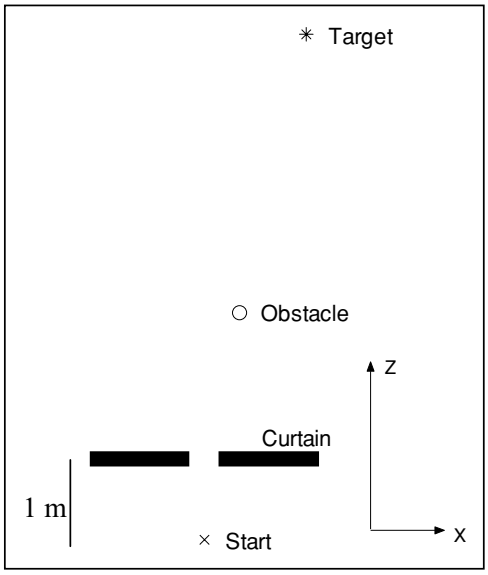

Fig. 1. Schematic of the object configuration, showing the +8° target angle, with the target at 8 m and the obstacle at 3 m (in the Z direction). Participants began each trial at X and walked through the gap in the curtain, around the obstacle to the target.

of differential equations, a *dynamical system*, whose solutions correspond to the observed behavioral trajectories in state space. Since the physical body has a moment of inertia, changing the direction of travel requires angular acceleration, implying that it must be at least a second-order system.

1.3.1 *Steering to a Goal.* To specify these equations, Fajen and Warren [2003] performed a series of experiments on human walking in an ambulatory virtual environment. In the first experiment, they observed that participants turn onto a straight path toward a stationary goal, with an angular acceleration that increases with the heading error and decreases with distance. They modeled this behavior as an angular "mass-spring" system. Intuitively, imagine that the agent's current heading direction is attached to the goal direction by a damped spring. The angular acceleration ($\ddot{\phi}$) of steering thus depends on the spring stiffness (k_g) and the heading error ($\beta_g = \phi - \psi_g$):

$$\ddot{\phi} = -b\dot{\phi} - k_g(\phi - \psi_g)(e^{-c_1 d_g} + c_2) \tag{1}$$

The "damping" term (b) resists turning, which tends to yield straight paths and reduce oscillations. The "stiffness" term (k_g) indicates that angular acceleration increases linearly with heading error. In addition, stiffness decreases exponentially with distance (d_g), where c_1 determines the rate of decay and c_2 a minimum angular acceleration for distant goals. Least-squares fits to the mean time series of heading yielded $b = 3.25$, $k_g = 7.50$, $c_1 = 0.40$, and $c_2 = 0.40$, with an average $R^2 = 0.98$ over all conditions. The model captured the mean steering behavior very well, with simulated locomotor paths that were very similar to the human data [Fajen and Warren 2003].

1.3.2 *Obstacle Avoidance.* Now consider the task of avoiding an obstacle. In Fajen and Warren's [2003] second experiment, participants turned away from the obstacle with an angular acceleration that decreased with both the obstacle-heading angle and obstacle distance. To model this behavior, imagine that the heading direction is repelled from the obstacle direction by another spring. Angular

acceleration thus depends on the spring stiffness (k_o) and the obstacle-heading angle ($\phi - \psi_o$):

$$\ddot{\phi} = -b\dot{\phi} + k_o(\phi - \psi_o)(e^{-c_3|\phi-\psi_o|})(e^{-c_4 d_o}) \quad (2)$$

The positive "stiffness" term indicates that angular acceleration decreases exponentially as the agent heads more to the left or right of the obstacle; the amplitude of this function is determined by k_o and its decay rate by c_3. The stiffness also decreases exponentially to zero with obstacle distance, where c_4 is the decay rate. Least-squares fits to the mean time series of the obstacle-heading angle yielded parameter values of $k_o = 198.0$, $c_3 = 6.5$, and $c_4 = 0.8$, with a mean $R^2 = 0.97$ over all conditions. Based on their third experiment, Fajen and Warren subsequently adjusted the c_4 parameter to 1.6; we will use that value here. The model thus captured the behavioral dynamics of obstacle avoidance and simulations reproduced the human paths quite closely. Adding 10% Gaussian noise into all perceptual variables and model parameters only induced a standard deviation of a few centimeters in the path's lateral position around an obstacle, demonstrating that the model is robust.

In more complex configurations of goals and obstacles, the model components are additively combined to predict behavior, with no additional parameters. In effect, a spring is added to the model for each object, and the current heading is the resultant of all spring forces acting on the agent at that moment. Locomotor routes thus emerge from the interaction of the agent and environment in an on-line fashion, rather than being explicitly planned in advance. Subsequently, a third component has been developed to model the interception of a moving target [Fajen and Warren 2004, 2005], as well as a fourth component for avoiding a moving obstacle [Cohen and Warren 2005]. The goal of this program of research is to determine whether human locomotor paths in complex dynamic environments can be predicted by linear combinations of these four elementary components.

A simpler hypothesis for steering to a stationary goal proposes that the agent holds the goal at a fixed eccentricity with respect to the locomotor axis, rather than bringing the heading error to zero [Rushton et al. 2002]. This generates paths in the form of equangular spirals, which increase in curvature at the end of the trajectory as the goal is approached. However, Fajen and Warren's [2003] data clearly show the opposite pattern, in which participants initially turn onto a straight path, with greater curvature at the beginning of the trajectory.

An alternative hypothesis proposes that the agent steers to cancel *target drift,* that is, to null the angular velocity of the goal with respect to the locomotor axis ($\dot{\beta}_g$) or a frame that is fixed to the locomotor axis [Llewellyn 1971; Rushton et al. 2002]. As formalized by Wilkie and Wann [2003], the model has only two parameters, analogous to a stiffness and damping terms, with no distance term. If one assumes a translational path of locomotion, target drift goes to zero ($\dot{\beta}_g = 0$) only when one is traveling on a straight path to the goal ($\beta_g = 0$). This is because, following the basic law of optic flow [Nakayama and Loomis 1974], the target's angular velocity is proportional to the sine of the target-heading angle and inversely proportional to distance. However, if the agent can turn as well as translate, nulling $\dot{\beta}_g$ also generates equiangular spiral paths to the goal that depend on initial conditions. Thus, apparently simpler models, based on fixed eccentricity or target drift, do not successfully reproduce human paths without additional parameters.

1.4 Locomotion in Real and Virtual Environments

In the present study, we compared locomotor paths in a virtual environment to those in a matched physical environment. The participant's task was to walk to a stationary goal while avoiding a stationary obstacle en route. The objects were vertical posts on a textured ground plane and their locations were varied from trial to trial.

The purpose of the experiment was twofold. First, we sought to assess the similarity of locomotor paths in real and virtual environments. On the one hand, previous evidence of large perceptual differences

between the two environments might lead one to expect large behavioral differences. One hypothesis is that, if an obstacle is known to be virtual and, hence, without physical consequences, participants might exhibit riskier behavior in virtual environments, such as allowing less clearance and more collisions with obstacles. Conversely, greater uncertainty about the scale, position, or character of virtual objects, or about the participant's own position in virtual space, could lead to larger deviations around obstacles. In addition, the 50% distance compression observed in virtual environments suggests the hypothesis that detours around an obstacle might be initiated earlier and lead to larger deviations.

On the other hand, there are also reasons to believe that locomotor behavior in real and virtual environments may be quite similar. The locomotor distance compression in virtual environments is largely eliminated by 5–7 min of adaptation with continuous visual feedback [Mohler et al. 2006]. Previous results suggest that visual–motor control in some tasks is not based on explicit perceptual judgments, but on task-specific control relations that may be comparable in both environments. To the extent that locomotor paths are similar in real and virtual environments, the use of virtual reality would be partially validated as a research tool for the study of human locomotion.

Second, we sought to assess how well the steering dynamics model generalizes from the virtual environment in which it was developed [Fajen and Warren 2003] to new virtual goal/obstacle configurations, as well as to a real environment with physical objects. Two levels of generality are considered: whether the present form of Eqs. (1) and (2) can capture mean behavior in new conditions and whether Fajen and Warren's [2003] specific parameter values can do so. A related question is whether individual differences in locomotor behavior can be accommodated by different parameter values in the model. Up to this point, the model has been fit to mean paths, but here we also perform separate parameter fits to each participant's data.

The observed locomotor paths were evaluated in two ways. First, we compared direct measurements of the paths themselves, including the curvature of the path around the obstacle, the deviation of the path from a straight line to the goal, and the passing distance from the obstacle. Second, we used the steering dynamics model to compare the entire path shape by fitting the model to the mean paths in each environment and comparing the resulting parameter values. Particular parameter differences may provide some insight into the locomotor strategies in real and virtual environments. For example, steering more directly to a goal might be reflected in both a higher "stiffness" parameter (k_g), which determines the attraction of the heading direction toward the goal direction (Eq. 1), and a slower decay rate of attraction with distance (c_1). Risky behavior in which a participant passes an obstacle with less clearance might be captured by a lower obstacle "stiffness" (k_o) or in an increase in the c_3 parameter, which determines the angular decay rate of the repulsion function and hence its lateral spread. Approaching closer to the obstacle before deviating might be expressed by an increase in the c_4 parameter (Eq. 2), which determines the decay rate of the repulsion function with distance.

2. METHOD

2.1 Participants

Ten college age participants, 6 female and 4 male, took part in the experiment. Informed consent was obtained before participation in the study.

2.2 Apparatus

The experiment was conducted in the Virtual Environment Navigation Lab (VENLab) at Brown University in an open 12 m × 12 m room. The task consisted of walking to a stationary target while avoiding a stationary obstacle, similar to Fajen and Warren's [2003] Experiment 2 (see Figure 1 for a schematic of the experimental conditions). Participants began each trial by walking through a 0.60-m wide gap in

a curtain, located 1 m from the starting position. The target, a green post (0.08 m radius; 2 m tall), was placed 8 m from the curtain (in the Z direction) at an angle from the initial direction of travel (-12, -8° to the left, or $+8$, $+12^\circ$ to the right); it was not visible through the curtain. The obstacle, a white post (0.08 m radius; 2 m tall), was placed either 3 or 5 m from the curtain (in the Z direction) and 3° closer to the initial direction of travel (e.g., if the target was at -12° the obstacle was placed at -9°).

Two environments were tested. In the virtual condition, participants viewed an immersive virtual environment that simulated the VENLab room, including the curtain 1 m from the starting location, the target post, and the obstacle post. It was presented in a Kaiser ProView-80 HMD (Kaiser Electro-Optics, Carlsbad, CA), with a 60° (horizontal) $\times$ 40° (vertical) binocular field of view and a resolution of 640×480 pixels in each eye. Stereo images of the three-dimensional (3D) environment were generated using an Onyx2 Infinite Reality workstation (SGI, Mountain View, CA) at a frame rate of 60 Hz, using WorldToolKit software (Sense8, Inc., San Rafael, CA). The participant's head position (4 mm RMS error) and orientation (0.1° RMS error) were measured using an IS-900 hybrid inertial/ultrasonic tracker (InterSense, Burlington, Massachussetts) at a sampling rate of 60 Hz and were used both to update the display and to collect data for analysis. Total latency was approximately 68 ms (4 frames), as determined by cross-correlation between the signals from two photodiodes, one mounted on the tracker reading a stationary gray-scale ramp, and the other mounted in the HMD reading a virtual ramp displayed on the HMD screen, as the HMD was translated by hand. The HMD cable was secured to a waist belt, and a "wrangler" followed the participant to handle the cable.

In the physical environment condition, participants viewed the actual room while walking around the VENLab wearing a bicycle helmet instead of the HMD. Head position and orientation were collected using the same tracker mounted on the helmet and the data were recorded for analysis. To match the virtual environment, a curtain was hung from the ceiling and target and obstacle posts were presented in identical positions. The posts were made of PVC pipe and were repositioned by hand between trials. The target, obstacle, curtain, and carpet in the virtual environment were approximately color matched to their physical counterparts.

2.3 Procedure

Before testing in the virtual condition, the lens separation in the HMD was adjusted to the participant's interocular distance. To check for stereoscopic fusion, a random-dot stereogram of a square was presented and further adjustments were made if necessary. Participants were instructed to walk normally to the green target while avoiding the white obstacle. Each participant performed one practice trial in each environment to demonstrate that they understood the task and were comfortable with the equipment. They were informed that they could take breaks between trials or stop entirely if they experienced symptoms of simulator sickness. No participants reported such symptoms or elected to discontinue the experiment.

The experiment had a 2 (environment) $\times$ 2 (target angle) $\times$ 2 (obstacle distance) $\times$ 2 (left/right direction) within-subject design. The virtual and physical environments were tested in separate sessions in a counterbalanced order. In each environment, five trials with each target/obstacle configuration were presented in a random order, for a total of 80 test trials. A session lasted approximately 45 min.

2.4 Data Analysis

Three metrics were computed on the path in the horizontal plane to characterize the participant's detour around the obstacle. First, the median[1] *radius of curvature* was computed along the full length

[1]The median radius of curvature was used rather than the mean radius of curvature to reduce problems caused by large radii that occur when the path is close to linear.

of the path from the curtain to the target. The radius of curvature (κ) at each point on the path was calculated as

$$\kappa = \frac{(\dot{X}^2 + \dot{Z}^2)^{1.5}}{(\dot{X}\ddot{Z} - \ddot{X}\dot{Z})} \tag{3}$$

where X and Z are head position coordinates in a horizontal plane and the median value was computed. This provides an estimate of the overall curvedness of the path, that is, its average departure from a straight path at all points. Second, the *maximum deviation* from a straight line between the gap in the curtain and the target was calculated for each trial. This provides an estimate of the deviation from a straight path at a point that is not necessarily adjacent to the obstacle. Third, the *minimum clearance* between the path and the obstacle was calculated. This provides a measure of the passing distance—how close the path came to the obstacle at its nearest point.

There were no order effects of the virtual and physical environments on these three metrics ($p > 0.2$), so the data were collapsed across order in subsequent analyses. To examine differences between conditions, a four-way repeated measures ANOVA (environment $\times$ target angle $\times$ obstacle distance $\times$ direction) was performed for each of the three metrics; to look at individual differences, these ANOVAs were repeated on each participant's data. The different target angles and obstacle distances were expected to influence the participant's path and, hence, to have an effect on each metric; tests of these main effects and interactions are included as a way of establishing that there is sufficient power to detect differences in behavior. A significant main effect of environment, or any interactions with environment, would indicate differences in behavior between the virtual and physical environments.

2.5 Model Parameter Fitting

Given that our goal was to model mean human behavior, a mean path was calculated in each experimental condition for the purpose of fitting the parameters of Fajen and Warren's [2003] steering dynamics model. The use of a mean path equated the duration and weight of each trial, and reduced the effects of measurement noise and intertrial variability. (We have also fit the trial data and observed that the parameter values are essentially unchanged.) First, because trial duration varied, we normalized the time-series data by calculating the mean position at 0.5-m intervals along the Z axis, from 0.5 m past the curtain to within 1.5 m of the target, yielding 13 data points per trial. This interval was deemed sufficient to capture the gradual change in lateral position over the course of a trial. For each interval, the sample in which the participant's Z position was closest to the specified Z position was found, and the corresponding X position was identified. The mean value of X was then computed for each interval in each condition, for each subject; grand means were computed across subjects.

Parameter values were found by a least-squares method that minimized the objective function

$$f(q) = \sum_{j=1}^{ncond} \sum_{i=1}^{13} (\hat{X}_{ij} - X_{ij})^2 \tag{4}$$

where q represents the parameters to be fit, X is the mean X value in the data for the 13 Z positions, $\hat{X}$ is the X value predicted by the model, and *ncond* is the number of conditions used in the parameter fitting. Parameters were fit using NOMAD, a generalized search program using MATLAB script [Abramson et al. 2004]. NOMAD searches in the neighborhood of the initial estimate for parameter values that find lower values of the objective function. The parameter fitting program was terminated and an optimal set of parameters was found when mesh size < 0.0001.

To examine differences between conditions, several different parameter searches were done with model speed constant at 1 m/s, as in Fajen and Warren [2003]. First, a series of parameter fits were

performed on the grand mean data across all participants, including one fit for all experimental conditions and then separate fits for the virtual environment and the physical environment alone. Second, to investigate individual differences, parameters were estimated separately for each participant in each environment. R^2 values were calculated for each of the parameter estimates using the following equations:

$$\begin{aligned} SSE &= \sum_{j=1}^{ncond} \sum_{i=1}^{13} \left(\hat{X}_{ij} - X_{ij}\right)^2 \\ SST &= \sum_{j=1}^{ncond} \sum_{i=1}^{13} \left(X_{ij} - \bar{X}_j\right)^2 \\ R^2 &= 1 - \left(\frac{SSE}{SST}\right) \end{aligned} \tag{5}$$

where X is the averaged X value in the data, $\hat{X}$ is the X value predicted by the model, $\bar{X}$ is the mean X from the averaged data for the experimental condition, and *ncond* is the number of conditions used in the calculation of the R^2 values.[2] When appropriate, R^2 values were compared statistically by applying a one-sided F test on the ratio between SSE terms, similar to a test comparing standard deviations between two samples.

3. RESULTS

Sample data for two participants appear in Figure 2, which presents paths for every trial in all target/obstacle configurations; solid red traces correspond to the physical environment and dashed blue traces to the virtual environment. Figure 2a shows a participant who exhibited little systematic difference between the virtual and physical environments. In contrast, the participant in Figure 2b displayed the greatest difference between the environments, as estimated by the root mean square error between the mean paths; the paths in the physical environment were straighter and did not deviate as much around the obstacle as those in the virtual environment. For many participants there appeared to be small, but systematic differences between the physical and virtual environments: their paths tended to deviate slightly earlier and farther around virtual obstacles than physical obstacles.

3.1 Radius of curvature

The median radius of curvature was not statistically different in the physical ($M = 1.09$ m, $SD = 0.20$ m) and virtual ($M = 1.17$ m, $SD = 0.10$ m) environments, $F(1, 9) = 2.47$, $p = 0.1505$, or in any interactions with environment. As expected, there was an influence of the object configuration, with significant main effects of target angle, $F(1, 9) = 21.96$, $p = 0.0011$, left/right direction, $F(1, 9) = 171.09$, $p < 0.001$, and their interaction, $F(1, 9) = 5.22$, $p = 0.0482$. Tukey post-hoc tests showed larger median radii of curvature (indicating straighter paths) with target angles of $\pm 8^\circ$ as compared to $\pm 12^\circ$ and on trials in which the target was placed to the right of the initial direction of movement. The significant interaction resulted from a smaller radius of curvature (i.e., a more curved trajectory) in the -12° condition than would be expected just from the main effects (see Figure 3). In the individual subject ANOVAs, a significant effect of environment was observed for only 4 out of 10 participants. Thus, the overall path curvature was comparable in physical and virtual environments.

[2]This calculation of R^2 is not identical to the R^2 value for a regression. Some of the assumptions in performing a fit of a linear model no longer hold, so that the familiar form of SSR + SSE = SST is not correct. Nevertheless, this approach gives a good measure of the amount of variability explained by the model.

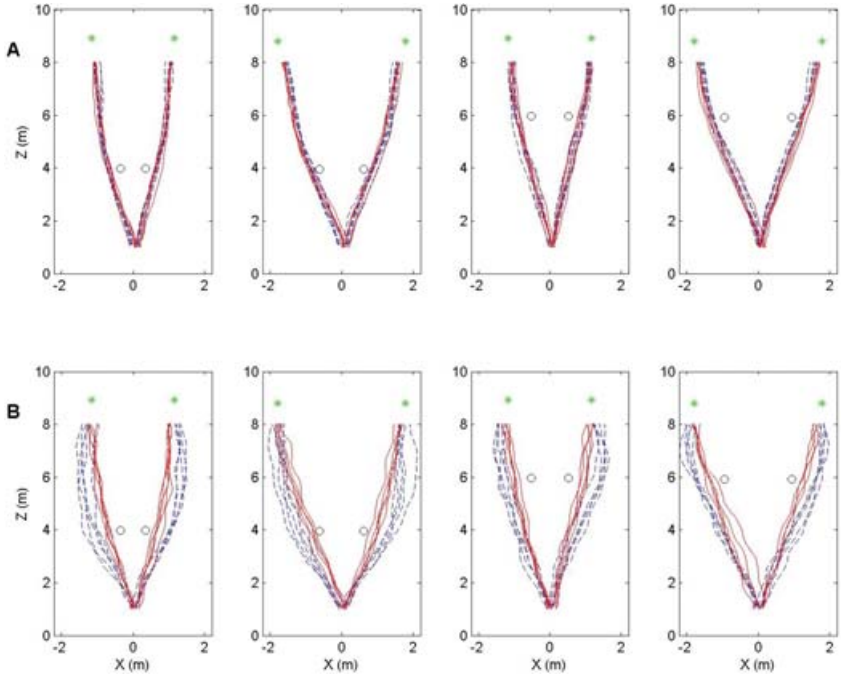

Fig. 2. Sample data from two participants, showing all paths in the four-object configurations (columns). Row A, A participant with similar paths in the physical and virtual environments. Row B, The participant with the greatest difference between environments. Abscissa is X direction (m) and ordinate is Z direction (m); units are not equal. Blue dashes, virtual environment; red solid, physical environment.

3.2 Maximum Deviation

In contrast, the maximum deviation from a straight path was slightly (by 0.16 m) but significantly greater in the virtual environment ($M = 0.59$ m, $SD = 0.17$ m) than in the physical environment ($M = 0.43$ m, $SD = 0.12$ m), $F(1, 9) = 10.35$, $p = 0.0105$. There was also a significant three-way interaction between target angle, direction, and obstacle distance, $F(1, 9) = 5.69$, $p = 0.0407$, which arose from larger deviations in the $+12^\circ$, 4 m and the -12°, 6 m obstacle configurations than with the other configurations. The individual subject ANOVAs revealed a significant effect of environment in 6 out of 10 participants. Thus, most participants deviated somewhat farther from a straight path to the target in the virtual than in the physical environment.

3.3 Minimum Clearance

A similar effect was observed for the minimum clearance from the obstacle, which was 0.16 m greater in the virtual environment ($M = 0.51$ m, $SD = 0.19$ m) than in the physical environment ($M = 0.35$ m, $SD = 0.15$ m), $F(1, 9) = 11.02$, $p = 0.0089$. There were also significant effects of object configuration, including target angle, $F(1, 9) = 9.02$, $p = 0.0149$, obstacle distance, $F(1, 9) = 49.12$, $p < 0.0001$, and direction, $F(1, 9) = 8.17$, $p = 0.0188$. In addition, there was a significant three-way interaction of target angle, obstacle distance, and direction, $F(1, 9) = 6.79$, $p = 0.0285$, stemming from a smaller minimum distance in the -12°, 4 m obstacle configuration than in the other configurations. The individual subject ANOVAs confirmed a significant effect of environment in 8 of the 10 participants. Thus, consistent with

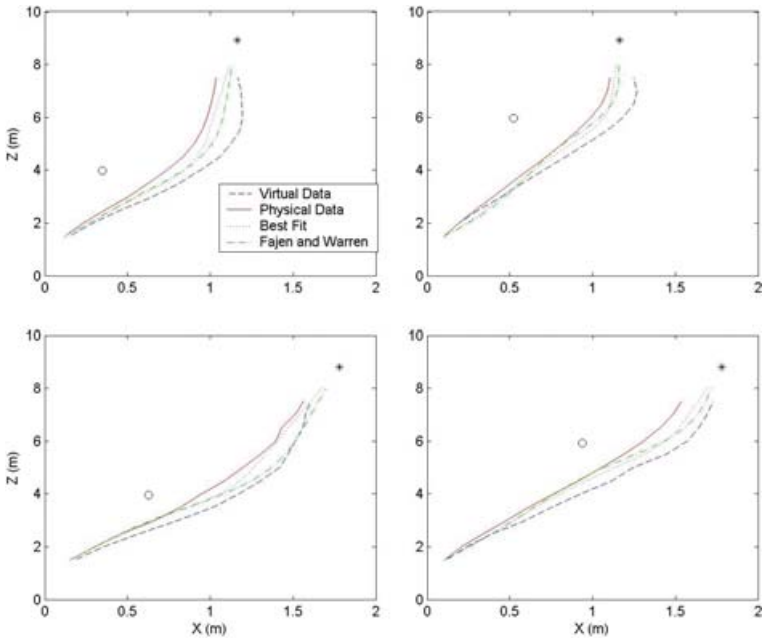

Fig. 3. Mean paths and overall model simulations for each object configuration (panels). Abscissa is X direction (m), ordinate is Z direction (m), and data are collapsed left/right. Blue dashes, virtual environment data; red solid, physical environment data; black dots, overall best-fit path; green dot–dashes, path generated with Fajen and Warren's [2003] parameters.

the maximum deviation measure, most participants passed slightly farther from virtual obstacles than physical obstacles.

3.4 Walking Speed

Participants walked slightly slower in the virtual (1.17 m/s $+/-$ 0.11 m/s) than the physical (1.30 m/s $+/-$ 0.12 m/s) environment $F(1, 9) = 19.36$, $p = 0.00017$).

3.5 Parameter Fitting

3.5.1 *Overall Fit.* We began by fitting the model to the data averaged across all participants, specifically to the mean path for each object configuration (i.e., both environments combined). The resulting parameter values and R^2 measures are presented in Table I; the best-fit path for each configuration (black dotted curve) appears in Figure 3, falling between the mean human paths in the physical (solid red curve) and virtual (blue dashed curve) environments. The overall goodness of fit was quite high, with $R^2 = 0.9597$. Comparable R^2 values were obtained when the same overall parameters were used to model the physical environment data ($R^2 = 0.9543$) separately from the virtual environment data ($R^2 = 0.9638$), $F(12, 12) = 1.26$, $p = 0.3477$. These results indicate that the model can approximate the data from both environments with a single set of parameters.

3.5.2 *Physical and Virtual Environments.* The model was then separately fit to the physical and virtual environment data (see Table I). The simulated paths for the physical (green dot-dash curve) and virtual (black dotted curve) environments closely match the corresponding mean human paths for each configuration (see Figure 4). The goodness of fit measure in each environment was significantly higher than that for the overall fit to the respective environment; for the virtual environment the R^2

Table I. Parameter Values and Associated R^2 for Model Fits to the Mean Paths in the Virtual (V) and Physical (P) Environments.[a]

	Overall Fit	V Data Fit	P Data Fit	V Data Fit (reduced)	P Data Fit (reduced)	Fajen and Warren
b	6.55	6.95	11.25	3.25	3.25	3.25
K_g	28.8	21.8	40.4	25.6	17.9	7.5
c_1	0.42	0.63	0.43	0.53	1.00	0.4
c_2	0.31	0.3515	0.334	0.40	0.40	0.4
K_o	50	51.75	51.75	198	198	198
c_3	3.5	3.45	3.45	6.88	11.34	6.5
c_4	0.6	0.575	0.575	1.01	1.06	1.6
Overall R^2	0.9597	—	—			0.9540
V Data R^2	0.9638	0.9886	0.9220	0.9825	0.9140	0.9513
P Data R^2	0.9543	0.7649	0.9838	0.7718	0.9810	0.9575

[a]V Data R^2 indicates the goodness of fit for the column parameters to the virtual environment data and P Data R^2 that for the column parameters to the physical environment data.

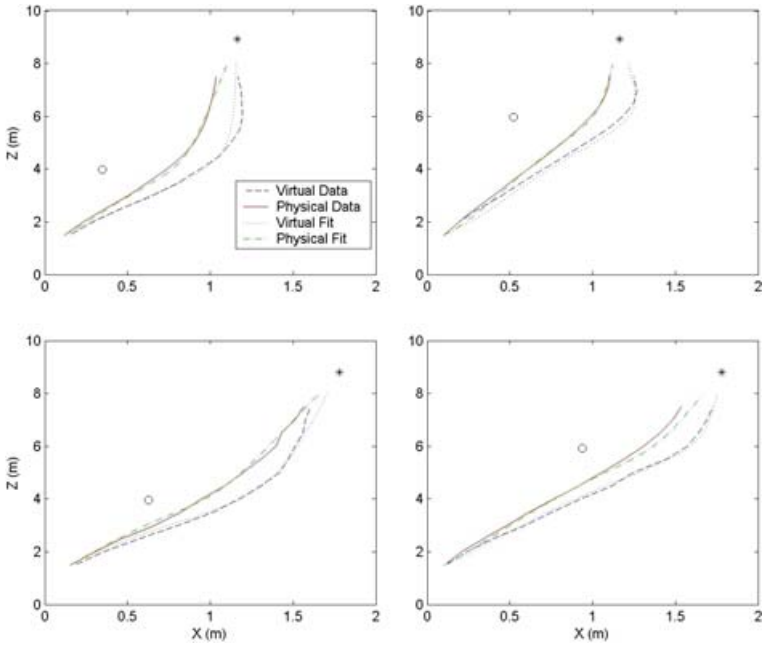

Fig. 4. Mean paths with separate model simulations for the virtual and physical environments (panels as in Figure 3). Blue dashes, virtual environment data; black dots, best-fit path to virtual data; red solid, physical environment data; green dot–dashes, best-fit path to physical data.

value rose to 0.9886, $F(12, 12) = 3.17$, $p = 0.0282$, while the R^2 for the physical environment increased to 0.9838, $F(12, 12) = 2.82$, $p = 0.0425$. In contrast, when the virtual parameters were used to model the data from the physical environment, the R^2 fell to 0.7649, $F(12, 12) = 5.14$, $p = 0.0041$; and when the physical parameters were used to model the virtual data, it slipped to 0.9220, $F(12, 12) = 2.75$, $p = .0463$. This confirms that there are small, but systematic, differences between paths in the two environments that can be captured by different parameter values. To investigate the source of these

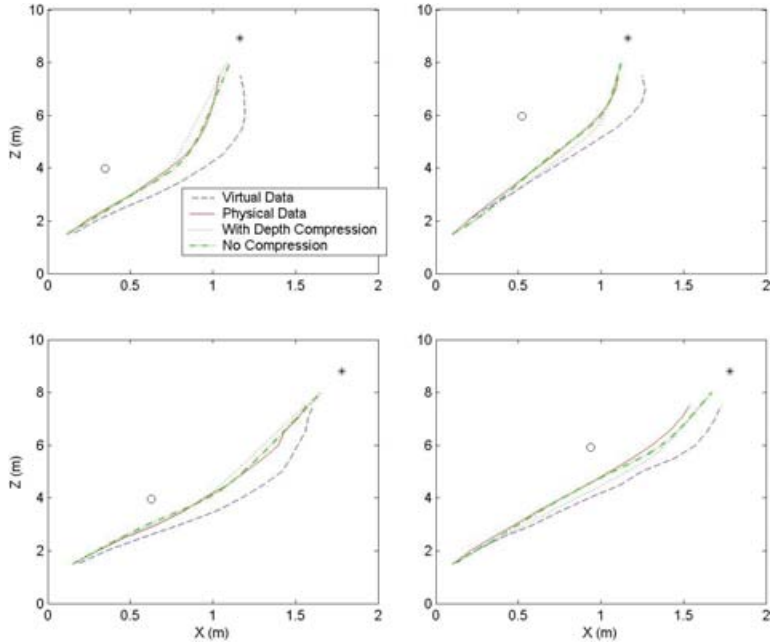

Fig. 5. Mean paths and overall depth compression simulations for each configuration (as in Figure 3). Blue dashes, virtual environment data; red solid, physical environment data; black dots, model path with 50% depth compression; green dot–dashes, best-fit path without depth compression.

differences, we explored the possibilities that they were influenced by the observed difference in walking speed or by depth compression in virtual reality.

3.5.3 *Walking Speed.* To assess whether the significant difference in walking speed might account for the different paths in virtual and physical environments, we repeated the fitting procedure using the mean speed for each environment in the model. The overall R^2 showed a small, but not significant, decline in fit ($R^2 = 0.9458$), $F(12, 12) = 1.34$, $p = 0.3101$, as did the separate goodness of fit to the virtual data ($R^2 = 0.9471$), $F(12, 12) = 1.46$, $p = 0.2611$ and the physical data ($R^2 = 0.9440$), $F(12, 12) = 1.23$, $p = 0.3628$. Thus, taking speed into account does not significantly improve the model fit to the data, suggesting that the difference between the physical and virtual paths is unlikely to be a consequence of walking speed.

3.5.4 *Distance Compression.* We then sought to determine whether a homogeneous distance compression of 50% could account for the larger path deviations in the virtual environment. To simulate paths through the virtual environment, we used model parameters from the physical environment but multiplied the input distances d_g and d_o by 0.5 on each time step. This effectively compressed the perceived egocentric distance to the target and obstacle by 50%; the visual environment thus gradually expanded in depth as the agent traveled through it. The results appear in Figure 5. Counterintuitively, the simulated paths with distance compression (black dots) are nearly identical to those with no compression (green dot–dashes), which are very close to the physical human data (red solid). Simulated compression creates only a marginal and not statistically significant improvement in the goodness of fit to the virtual human data ($R^2 = 0.9307$), compared to no compression ($R^2 = 0.9220$), $F(12, 12) = 1.13$, $p = 0.4179$. Simulations with other compression values yielded similarly small effects; we will consider

the reasons for this finding in the discussion. This result suggests that distance compression by itself does not account for the larger deviations observed in the virtual environment.

3.5.5 *Fajen and Warren Parameters.* To determine how well Fajen and Warren's [2003] original parameter values generalize to new object configurations in a virtual environment, as well as a corresponding physical environment, we simulated the model with parameter values from their experiment 3. The simulated paths (green dot–dashes) in Figure 3 lie in between the mean physical and virtual data, close to the overall best-fit path (black dots). The goodness of fit to the full data set ($R^2 = 0.9540$) is not significantly different from the fit to the physical environment data ($R^2 = 0.9575$), the virtual environment data ($R^2 = 0.9513$), or the current overall fit with free parameters ($R^2 = 0.9597$) ($p > 0.05$ for all comparisons; see Table I). Thus, it appears that Fajen and Warren's parameters generalize to new virtual configurations as well as to corresponding physical configurations, again demonstrating that the model can approximate data from both environments with a single set of parameters.

3.5.6 *Reduced Model.* The fact that the parameter values from the present overall fit are somewhat different from Fajen and Warren's values despite similarities in the quality of fit indicates that the data can be closely approximated by different combinations of parameters. That is to say that the parameter set contains redundancies, such that various parameter combinations produce highly similar paths. This suggests that the original model may contain more free parameters than minimally necessary to account for the human data in this experiment. To investigate this question, we determined how well a reduced parameter set would capture the observed differences between the physical and virtual environments. First, we fixed the "damping" parameter b on the assumption that it reflects the physical resistance to turning (e.g., opposed by the centripetal force required to displace the body mass on a curved path). Second, we fixed the goal's c_2 parameter because it is a constant that simply ensures a minimum goal attraction at large distances. Third, we fixed the obstacle stiffness parameter k_o, which specifies the amplitude of the repulsion function, because it is redundant with parameter c_3, which affects both the amplitude and the spread of the repulsion function; as long as k_o has a high value, c_3 determines the agent's deviation around the obstacle. These three parameters were thus held constant at Fajen and Warren's values ($b = 3.25$, $c_2 = 0.4$, $k_o = 198$) while the remaining four parameters were free to vary. Despite the reduced number of free parameters, the fits remained quite strong ($R^2 = 0.9825$ for the virtual and $R^2 = 0.9810$ for the physical environment), with no significant differences compared to the full model ($F(12, 12) = 1.54$, $p = 0.2328$ for the virtual environment and $F(12, 12) = 1.17$, $p = 0.3950$ for the physical environment). This result implies that the reduced model is sufficient to account for the observed differences between the two environments.

3.5.7 *Individual Fits.* Given that the reduced model fit the group data well, we used it as a window onto individual differences in performance. The reduced parameter set was separately fit to each participant's mean data in all configurations, for both the virtual and the physical environment (see Table II). With the exception of participant 4 in the physical environment, the fits were very strong, ranging from $R^2 = 0.9595$–0.9977, indicating that the reduced model is sufficient to capture individual differences. Wilcoxon signed-rank sum tests were applied to each parameter to identify differences between environments. Significant differences between environments were found in c_1 ($T^* = 2$, $p < 0.005$), and c_3 ($T^* = 1$, $p < 0.005$), while k_g approached but did not reach significance ($T^* = 46$, $p = 0.064$). The c_1 parameter, the rate of decay in attraction with distance, was larger in the physical environment than in the virtual environment, meaning that participants tended to turn faster toward the goal in the virtual environment at a given distance. This is reflected in more rapid turns after the virtual obstacle is passed (Figure 4); the marginally higher stiffness (k_g) in the virtual environment would also contribute to this effect. A corresponding difference did not occur in the c_4 parameter, the rate of decay in obstacle

Table II. Parameter Fits for the Reduced Parameter Model and the Associated R^2 Values for Each Participant in the Virtual (V) and Physical (P) Environments.

	Kg		c_1		c_3		c_4		R^2	
	V	P	V	P	V	P	V	P	V	P
1	42.05	34.78	0.0950	0.1041	2.681	3.250	0.600	0.600	0.9793	0.9903
2	29.83	15.69	0.1963	0.4200	2.950	9.563	0.600	0.984	0.9689	0.9752
3	50.00	27.81	0.0575	1.1519	2.347	22.700	0.616	0.594	0.9871	0.9595
4	50.00	50.00	0.1044	0.2700	2.525	4.756	0.600	1.400	0.9695	0.6514
5	50.00	15.54	0.2122	0.5222	3.234	15.413	0.600	0.638	0.9812	0.9906
6	49.98	16.65	0.1575	1.1078	2.338	17.159	0.638	0.869	0.9787	0.9977
7	10.29	32.44	0.2113	2.0000	13.188	13.084	0.959	0.884	0.9940	0.9951
8	50.00	13.80	0.0000	2.0000	1.938	30.000	0.613	0.250	0.9895	0.9721
9	50.00	34.68	0.0569	0.9500	2.331	7.959	0.725	1.216	0.9697	0.9937
10	35.55	37.68	0.6550	0.5822	7.000	7.956	1.200	1.694	0.9884	0.9967
Mean	41.77	27.91	0.1746	0.9108	4.0532	13.184	0.7151	0.9129	0.9806	0.9522

repulsion with distance. In contrast, the c_3 parameter, the lateral decay in obstacle repulsion, was higher in the physical than the virtual environment; hence, the participant was repelled laterally from virtual more than from physical obstacles. This reflects the finding that participants tend to deviate on a wider path around obstacles in the virtual environment.

4. DISCUSSION

The present results indicate that there is a small, but reliable, difference in locomotor behavior between real and virtual environments. A majority of participants tended to detour slightly farther around an obstacle in the virtual environment than in the matched physical environment. On the other hand, the mean difference in the maximum deviation was only 0.16 m—approximately one head width—and 40% of participants exhibited no such difference (Figure 2a). In addition, the overall shapes of the physical and virtual paths were qualitatively similar (Figure 3) with no statistical difference in the median path curvature. The fact that the overall parameter fit yielded R^2 values above 0.95 with both the virtual and the physical data indicates that the paths can be closely approximated with a single set of parameter values.

This pattern of results leads us to conclude that virtual environments provide a valuable research tool for the study of visually guided locomotion, particularly when experimental manipulation of the real environment is prohibitive. The qualitative behavioral patterns are sufficiently similar to permit tests of theoretical questions in virtual environments, although quantitative details such as specific clearance distances and parameter values may have to be adjusted for a physical environment.

The residual difference in locomotor behavior between real and virtual environments presents something of a puzzle. First, the hypothesis that people display riskier behavior with virtual objects appears to be ruled out by the fact that the obstacle clearance is actually greater in the virtual environment than in the physical one. Second, the small difference in walking speed between the two environments ($\Delta = 0.13$ m/s) does not appear to account for the path difference, because adjusting the model speed does not significantly improve the fit to the data. Thus, if we take the model to be an adequate characterization of locomotor behavior, it implies that the difference between virtual and physical paths is not explained by walking speed. Third, the results also undermine the hypothesis that the path difference is a result of the 50% underestimation of distance in virtual environments. Surprisingly, model simulations that incorporated a 50% distance compression generated paths that were nearly identical to those with no compression. When combined with Mohler et al's (2006) finding that distance compression in a virtual environent is nearly eliminated by a short period of adaptation with continuous vision,

the results cast doubt on bias in distance perception as an explanation for differences in locomotor paths.

Why does such a large distance compression have a negligible effect on the simulated paths, given that the model contains distance terms? In the model, the agent's heading at any point results from competition between the heading direction's attraction toward the goal direction and its repulsion away from the obstacle direction. The attraction and repulsion functions both decay gradually with distance at similar rates, such that they are nearly parallel. A proportional compression in the goal and obstacle distances thus yields a proportional increase in both the attraction and repulsion, essentially preserving their ratio. The slight differences between the paths in Figure 5 derive from small differences between the exponential decay functions. Hence, to the extent that the model adequately represents locomotor dynamics, the simulations imply that the difference between virtual and physical environments cannot be attributed to distance compression. However, the model does predict an effect of distance underestimation when there is only a single goal in the scene (greater turning rate toward the target when depth is compressed), for, in that case, the attraction is not balanced by repulsion. This is evident in simulated paths after the obstacle is passed (Figure 5).

Finally, the analysis of individual fits using the reduced model suggests that the source of differences between the environments is twofold. First, the decay rate in lateral repulsion from the obstacle (c_3) was smaller in the virtual than the physical environment. This results in a larger maximum deviation and obstacle clearance, as observed in virtual environment. Such a parameter difference could reflect greater uncertainty about the location of an obstacle relative to the observer's own position in the virtual than the physical world. This might be a consequence of the reduced field of view in the HMD (60° H), or the fact that the observer's body (e.g., feet on the ground, distance of hands) was not visibly represented in the virtual world. Second, the decay in attraction to the goal with distance (c_1) was smaller in the virtual than in the physical environment, resulting in a faster turning rate toward the goal; a marginally higher goal stiffness (k_g) would also contribute to faster turning. This is observable as a more rapid turn after the obstacle is passed in the virtual environment. Taken together, these results suggest that the larger detour and sharper turn in the virtual environment might stem from a combination of greater lateral repulsion from the obstacle, perhaps because of uncertainty about its egocentric location and greater attraction to the goal direction in the virtual environment. These differences, although small, can be captured by parameter settings in the model. Individual differences in preferred paths can also be interpreted in terms of differences in the same three parameters.

The second motivation for the present study was to determine whether Fajen and Warren's [2003] steering dynamics model generalizes to new conditions. The results show that the model successfully transfers to new object configurations, environments, and participants, at two levels of generality. At an abstract level, the functional form of the second-order system, which, in essence, steers to a goal by nulling heading error ($\beta = \phi - \psi$) (Eq. 1) and avoids obstacles, via repulsion from the null point (Eq. 2), was sufficient to fit the mean paths in all configurations with R^2 values better than 0.98 in the virtual and physical environments. Moreover, the simulated paths closely reproduced the shapes of the mean paths in most conditions (Figure 4).

At the parametric level, the model also generalizes to new conditions with fixed parameters. Fajen and Warren's [2003] original parameter values modeled the present data ($R^2 = 0.9540$) nearly as well as the current overall best fit ($R^2 = 0.9597$), and yielded R^2 values better than 0.95 in each environment. The simulated paths fall between the current virtual and physical data and are nearly congruent with the current overall best-fit paths (Figure 3). Thus, the steering dynamics model can successfully predict human behavior with new object configurations, environments, and participants, without free parameters.

It is interesting to note that the significant statistical effects of the object configuration on obstacle clearance fall out naturally from the steering dynamics model, as can be seen in Figure 4. Taken together with the significant effect of target and obstacle position for radius of curvature, minimum clearance, and maximum deviation, this result suggests that obstacle clearance is not determined by a fixed personal space or safety margin for stationary obstacles in each participant, but rather depends on the configuration of start, obstacle, and goal positions. In the present account, what is commonly thought of as a zone of "personal space" [Gérin-Lajoie et al. 2005] is viewed as an emergent property of the dynamic interplay of attraction and repulsion forces in a particular object configuration.

It is important to point out that, even though the steering dynamics model has a number of free parameters, it is not completely general. The model cannot be fit to any arbitrary locomotor path, but generates a restricted family of humanlike paths. As described in the introduction, apparently simpler models fail to successfully capture human steering to a goal and would require additional terms to be extended to obstacle avoidance. Moreover, the present simulation results demonstrate that the original set of seven free parameters in Fajen and Warren's [2003] model can be effectively reduced to four (two for goals and two for obstacles) and still fit the range of paths in present data. The reduced model captures the differences between virtual and physical environments with R^2 values above 0.98 and differences between individual participants with R^2 values above 0.95. Thus, the model describes human steering dynamics with high accuracy even with a reduced parameter set. Most importantly, the fact that Fajen and Warren's [2003] original model can account for paths in new conditions with fixed parameters renders it not merely descriptive but predictive. Our current program of research determines whether the model can scale to more complex situations by linearly combining object components with no free parameters.

In summary, despite a small quantitative difference in the deviation around an obstacle, human paths in real and virtual environments are qualitatively similar in shape and can be closely fit with a fixed set of model parameters. We conclude that these results justify taking advantage of virtual environments to test hypotheses about locomotor behavior, with the caveat that specific details may need to be adjusted for physical environments.

REFERENCES

Abramson, M. A., Audet, C., and Dennis, J. E. 2004. Generalized pattern searches with derivative information. *Mathematical Programming 100*, 3–25.

Aglioti, S., Desouza, J. F. X., and Goodale, M. A. 1995. Size-contrast illusions deceive the eye but not the hand. *Current Biology. 5*, 679–685.

Beall, A. C., Loomis, J. M., Philbeck, J. W., and Fikes, T. J. 1995. Absolute motion parallax weakly determines visual scale in real and virtual environments. *Proceedings of the SPIE 2411*, 288–297.

Cohen, J. A. B., H. and Warren, W. H. 2005. Switching behavior in moving obstacle avoidance. *Journal of Vision 5*, 312a.

Creem-Regehr, S. H., Willemsen, P., Gooch, A. A., and Thompson, W. B. 2005. The influence of restricted viewing conditions on egocentric distance perception: Implications for real and virtual indoor environments. *Perception 34*, 191–204.

Dixon, M. W., Wraga, M. J., Proffitt, D. R., and Williams, G. C. 2000. Eye height scaling of absolute size in immersive and nonimmersive displays. *Journal of Experimental Psychology: Human Perception and Performance*, 582–593.

Fajen, B. R. and Warren, W. H. 2003. Behavioral dynamics of steering, obstacle avoidance, and route selection. *Journal of Experimental Psychology: Human Perception and Performance 29*, 343–362.

Fajen, B. R. and Warren, W. H. 2004. Visual guidance of intercepting a moving target on foot. *Perception 33*, 689–715.

Fajen, B. R. and Warren, W. H. in press. Behavioral dynamics of intercepting a moving target. Experimental Brain Research.

Franz, V. H. 2003. Planning versus online control: dynamic illusion effects in grasping? *Spatial Vision 16*, 211–223.

Franz, V. H., Gegenfurtner, K. R., Bülthoff, H. H. and Fahle, M. 2000. Grasping visual illusions: No evidence for a dissociation between perception and action. *Psychological Science 11*, 20–25.

Gérin-Lajoie, M., Richards, C. L., and Mcfadyen, B. J. 2005. The negotiation of stationary and moving obstructions during walking: Anticipatory locomotor adaptations and preservation of personal space. *Motor Control 9*, 242–269.

GLENNERSTER, A., TCHEANG, L., GILSON, S. J., FITZGIBBON, A. W., AND PARKER, A. J. 2006. Humans ignore motion and stereo cues in favor of a fictional stable world. *Current Biology 16*, 428–432.

GLOVER, S. AND DIXON, P. 2001. Dynamic illusion effects in a reaching task: Evidence for separate visual representations in the planning and control of reaching. *Journal of Experimental Psychology: Human Perception and Performance 27*, 560–572.

LLEWELLYN, K. R. 1971. Visual guidance of locomotion. *Journal of Experimental Psychology 91*, 224–230.

LOOMIS, J. M. AND KNAPP, J. M. 2003. In *Virtual and Adaptive Environments*. L. J. Hettinger and M. W. Haas, (Eds.) Lawrence Erlbaum, Mahwan, NJ. 21–46.

MESSING, R. M. AND DURGIN, F. H. 2005. Distance perception and the visual horizon in head-mounted displays. *Transactions on Applied Perception 2*, 234–250.

MILNER, A. D. AND GOODALE, M. A. 1995. *The Visual Brain in Action*. Oxford University Press, Oxford, England.

MOHLER, B. J., CREEM-REGEHR, S. H., AND THOMPSON, W. B. 2006. The influence of feedback on egocentric distance judgments in real and virtual environments. Unpublished manuscript.

NAKAYAMA, K. AND LOOMIS, J. M. 1974. Optical velocity patterns, velocity sensitive neurons, and space perception: A hypothesis, *Perception 3*, 63–80.

OOI, T. L., WU, B., AND HE, Z. J. 2001. Distance determined by the angular declination below the horizon. *Nature London 414*, 197–200.

OPITZ, D., GEGENFURTNER, K. R., AND BÜLTHOFF, H. H. 1996. A comparison of grasping real and virtual objects. *Perception 25 (Suppl.)*, 92–93.

PHILBECK, J. W. 1997. Comparison of two indicators of perceived egocentric distance under full-cue and reduced-cue conditions. *Journal of Experimental Psychology: Human Perception and Performance 23*, 72–85.

RUSHTON, S. K., WEN, J., AND ALLISON, R. S. 2002. *Proceedings Lecture Notes in Computer Science, 2525*. Springer–Verlag, Berlin. 576–591.

SAHM, C. S., CREEM-REGEHR, S. H., THOMPSON, W. B., AND WILLEMSEN, P. 2005. Throwing versus walking as indicators of distance perception in similar real and virual environments. *ACM Transactions on Applied Perception 2*, 35–45.

SCHÖNER, G., DOSE, M., AND ENGELS, C. 1995. Dynamics of behavior: Theory and applications for autonomous robot architectures. *Robotics and Autonomous Systems 16*, 213–245.

SEDGWICK, H. 1980. In *The Perception of Pictures*, M. A. Hagen, Ed. Academic Press, New York. 1.

SMEETS, J. B. J. AND BRENNER, E. 1999. A new view on grasping. *Motor Control 3*, 237–271.

SMEETS, J. B. J., GLOVER, S., AND BRENNER, E. 2003. Modeling the time-dependent effect of the Ebbinghaus illusion on grasping. *Spatial Vision 16*, 311–324.

TARR, M. AND WARREN, W. H. 2002. Virtual reality in behavioral neuroscience and beyond. *Nature Neuroscience, 5 (Suppl.)*, 1089–1092.

THOMPSON, W. B., WILLEMSEN, P., GOOCH, A. A., CREEM-REGEHR, S. H., LOOMIS, J. M., AND BEALL, A. C. 2004. Does the quality of the computer graphics matter when judging distances in visually immersive environments?, *Presence 13*, 560–571.

VISHTON, P. M., REA, J. G., CUTTING, J. E., AND NUNEZ, L. N. 1999. Comparing effects of the horizontal-vertical illusion on grip scaling and judgment: Relative versus absolute, not perception versus action. *Journal of Experimental Psychology: Human Perception and Performance 25*, 1659–1672.

WARREN, W. H. AND WHANG, S. 1987. Visual guidance of walking through apertures: Body scaled information for affordances. *Journal of Experimental Psychology: Human Perception and Performance 13*, 371–383.

WILKIE, R. M. AND WANN, J. 2003. Controlling steering and judging heading: Retinal flow, visual direction, and extra-retinal information. *Journal of Experimental Psychology: Human Perception and Performance 29*, 363–378.

WILLEMSEN, P., COLTON, M. B., CREEM-REGEHR, S. H., AND THOMPSON, W. B. 2004. *ACM SIGGRAPH Symposium on Applied Perception in Graphics and Visualization*. Los Angeles, CA. 35–38.

Received December 2005; revised October 2006; accepted December 2006